UDC 630*813

THERMAL ANALYSIS AND PYROLYSIS-GAS CHROMATOGRAPHY/MASS SPECTROMETRY OF FOSSIL WOOD FROM OF BÜKKÁBRÁNY, HUNGARY

O. A. Shapchenkova[1], S. R. Loskutov[1], M. A. Plyashechnik[1], Z. Pásztory[2]

[1] *V. N. Sukachev Institute of Forest, Russian Academy of Science, Siberian Branch*
Federal Research Center Krasnoyarsk Scientific Center, Russian Academy of Sciences, Siberian Branch
Akademgorodok, 50/28, Krasnoyarsk, 660036 Russian Federation

[2] *University of Sopron*
Bajcsy-Zsilinszky 4, Sopron, H-9400 Hungary

E-mail: shapchenkova@mail.ru, lsr@ksc.krasn.ru, lilwood@ksc.krasn.ru, pasztory.zoltan@uni-sopron.hu

Received 04.05.2022 г.

Fossil wood that is ca 7 million years old from Bükkábrány (Hungary) was analyzed by thermogravimetry (TG), differential scanning calorimetry (DSC) and pyrolysis-gas chromatography/mass spectrometry (Py-GC/MS) to evaluate alterations of its chemical composition. A wood sample of bald cypress (*Taxodium distichum* (L.) Rich.) from West Hungary was taken as a reference. The fossil wood was characterized by higher contents of total carbon (58.05 %) and total nitrogen (0.44 %) compared to recent wood. TG of fossil wood showed a high heterogeneity of wood substance, significant loss of polysaccharides and enrichment by lignin including more thermally stable components (> 500 °C). The enthalpy change (ΔH) of combustion (thermo-oxidation) for fossil wood was significantly higher than for recent wood (–18.17 kJ/g vs. –11.41 kJ/g). Py-GC/MS analysis of fossil wood showed a significant depletion of polysaccharide pyrolysis products and an increase in lignin pyrolysis products compared to recent wood. The pyrolytic H/L ratio indicates a preferential loss of polysaccharides in fossil wood. Polysaccharide pyrolysis products were rare and represented mainly by levoglucosan. Lignin also underwent substantial changes. A dramatic decrease in monomers, an increase in short side chain compounds and the presence of demethylated/demethoxylated compounds in the composition of lignin pyrolysis products are indicative of lignin alteration (degradation). Moreover, a high abundance of styrene, cresols, phenol and phenolic compounds was observed.

Keywords: *thermogravimetry, differential scanning calorimetry, analytical pyrolysis, evaluation of chemical composition alterations of fossil wood, bald cypress (Taxodium distichum (L.) Rich.), Western Hungary.*

How to cite: *Shapchenkova O. A., Loskutov S. R., Plyashechnik M. A., Pásztory Z.* Thermal analysis and pyrolysis–gas chromatography/mass spectrometry of fossil wood from the locality of Bükkábrány, Hungary // *Sibirskij Lesnoj Zurnal* (Sib. J. For. Sci.). 2022. N. 5. P. 56–69 (in English with Russian abstract).

DOI: 10.15372/SJFS20220505

INTRODUCTION

Fossil woods are always of great scientific interest because they can provide information about palaeoclimate, palaeoecology, phytogeography and evolution (Guleria, Awasthi, 1997). In the summer of 2007, a fossil forest was discovered in the opencast lignite mine near the village of Bükkábrány (Hungary). Catastrophic flooding of Lake Pannon and subsequent burial by deposition of sand from a prograding delta 7 million years ago preserved the Bükkábrány forest (Miocene epoch). The tree trunks were found standing in an upright position partly with bark and rather intact. The fossil forest at Bükkábrány is the only location in the world where large trees are preserved standing, in the original forest structure, as wood (Kázmér, 2008). The fossil trees have been identified as *Taxodio-*

xylon germanicum and *Glyptostroboxylon* (Erdei et al., 2009; Gryc, Sakala, 2010). The structure of the Bükkábrány forest was described by M. Kázmér (2011). Mummification is considered to be a potential mechanism of a remarkable preservation state of the fossil trees from Bükkábrány (Bardet, Pournou, 2015). A good preservation is a result of inhibition of wood-destroying microbes, decreased oxygen availability, and the absence of harsh chemical or physical conditions (Mustoe, 2018).

Although remaining well preserved, wood tissue has undergone decay, however the petrifaction process was not progressed, and that is why the tree kept its wood features. M. Bardet and A. Pournou (2015) and K. Nikoloui et al. (2016) examined the fossil wood samples from Bükkábrány using light and scanning electron microscopy and observed extended wood biodeterioration caused by bacteria (erosion and tunneling bacteria) and fungi.

The study of chemical composition of six samples taken from standing fossil trunks done by M. Hámor-Vidó et al. (2010) revealed lower contents of cellulose and total phenols than in intact recent trees. The authors suggested that redox potential and dissolved phenol content saturated water contributed to reduce microbial activity and preserve wood tissues. The loss of cellulose and degradation of lignin to some extent in fossil wood from Bükkábrány were detected by A. Bardet and A. Pournou (2015) by examining its chemistry with ^{13}C CPMAS NMR. They found that all signals assigned to cellulose have almost disappeared. Lignin degradation was more significant at the bottom than at the top or in the middle of the fossil trunk studied. FTIR spectra of the Bükkábrány samples also showed that peaks attributed to hemicellulose and cellulose at 1734 cm^{-1}, 1160 and 892 cm^{-1} disappeared and peaks related to aromatic vibrations in lignin at 1605 cm^{-1}, 1510, 1420 and 1267 cm^{-1} displayed higher intensity (Nikoloui et al., 2016).

It is known that in waterlogged environments, anaerobic bacteria and soft rot fungi, which attack mainly cellulose and hemicelluloses and modify the lignin in the cell middle lamella but do not degrade it completely, can slowly degrade wood. The waterlogged wood is often characterized by a good preservation but it can still be extensively degraded, poor in polysaccharides and mainly composed of residual lignin (Łucejko et al., 2015). In order to understand more about the extent of degradation of fossil wood from Bükkábrány, we used thermal analysis and analytical pyrolysis. The successful use of thermogravimetry (TG), differential scanning calorimetry (DSC) and pyrolysis-gas chromatography/mass spectrometry (Py-GC/MS) to study waterlogged archaeological, ancient and fossil woods has been demonstrated in a number of works (Tomassetti et al., 1987; Campanella et al., 1991; Obst et al., 1991; Colombini et al., 2007; Budrugeac, Emandi, 2010; Donato et al., 2010; Cavallaro et al., 2011; Tamburini et al., 2014, 2016; Łucejko et al., 2015; Traoré et al., 2017; Romagnoli et al., 2018). Thermal analysis provides information about the physical or chemical changes associated with substances, including wood and its components, as a function of temperature. Py-GC/MS is a precious tool to determine the chemical composition of all the wood constituents and to indicate the mechanisms of degradation reactions (Van Bergen et al., 2000; Tamburini et al., 2014; Ghalibaf et al., 2019). Therefore, the aim of this work was to evaluate the chemical alterations in main structural components (polysaccharides and lignin) of fossil wood from the Bükkábrány mine using TG, DSC, and Py-GC/MS.

MATERIAL AND METHODS

Wood material. The small pieces of a fossil trunk identified as *Taxodioxylon germanicum* were kindly provided by University of Sopron. The origin of the samples was the lignite mine of Bükkábrány (in the north-east part of Hungary). The trunks were discovered in a standing position, which proves the original location of the trees. The height of the fossil trunks was about three to five meters, and the upper parts of the trunks were missing. Presumably these parts were above the sediment and degraded in a short time. Water and the sediment shut off oxygen, preventing the degradation process preserving the wood for a long time. An average wood sample prepared from pieces of a fossil trunk was examined in this study. The wood sample of a closer relative recent bald cypress (*Taxodium distichum* (L.) Rich.) growing in Sopron (West Hungary), was taken as a reference. It was possible because this tree species still exists mostly in swampy territories. The wood samples were sawed with a fine-tooth metal saw to obtain fine sawdust. The powdered samples were used for TG, DSC, and Py-GC/MS.

Methods. Microscopic examination of fossil wood samples was done with a scanning electron microscope (TM-1000, Hitachi) equipped with an energy-dispersive X-ray microanalysis unit (EDX). The transverse and longitudinal sections were cut by hand. Observations were carried out at magnifications of 250–3000x.

Carbon and nitrogen contents in fossil and recent wood samples were determined with an ele-

mental analyzer (Vario ISOTOPE Cube, Elementar Analysensysteme GmbH).

Thermogravimetry was conducted on a TG 209 F1 thermal analyzer (Netzsch, Germany) in an air atmosphere with the gas flow of 20 mL/min from 25 to 700 °C, at 10 °C/min heating rate, in a corundum crucible (Al_2O_3). The enthalpy change (ΔH) of thermo-oxidative degradation of wood was determined by DSC. Differential scanning calorimetry was done with a DSC 204 F1 thermal analyzer (Netzsch, Germany) in an air atmosphere in the following conditions: temperature range 25–590 °C, the gas flow 40 mL/min, the heating rate of 10 °C/min, an aluminum pan with pierced lid.

Py-GC/MS analysis was performed using a multi-shot pyrolizer EGA/Py-3030D (Frontier Lab) attached to a GCMS-QP2020D (Shimadzu). Approximately 100 μg of sample were pyrolyzed at 600 °C. The gas chromatograph was equipped with a stainless steel Ultra Alloy-5 capillary column (30 m × 0.25 mm × 0.25 mm, liquid phase: 5 % diphenyl 95 % dimethylpolysiloxane). Oven temperature was held at 50 °C for 5 min and then increased to 240 °C at the rate 4 °C/min, and from 240 to 300 °C at the rate 10 °C/min, afterwards the final temperature of 300 °C was held for 5 min. The carrier gas was helium with a flow 1 ml/min. The split ratio was adjusted to 50. The mass spectrometer operated at ionization energy of 70 eV, an ion source temperature of 250 °C, in a scan range of m/z 40–550. The pyrolysis products were identified by comparison with the NIST mass spectral library and data published the literature (Pouwels et al., 1987; Stankiewicz et al., 1997; Łucejko et al., 2009; Traoré et al., 2016, 2017; Subagyono et al., 2021). The relative abundance of every compound was expressed as a percentage of the total peak area.

RESULTS AND DISCUSSION

Microscopic observations. The scanning electron microscopy (SEM) images of the fossil wood samples are shown in Fig. 1.

The anatomical features were well visible. Tracheids and ray parenchyma cells with deposits were seen (Fig. 1, *a*, *b*). Fungal hyphae and spores were found (Fig. 1, *c*, *d*). In a longitudinal section, erosion troughs (stripes) oriented along the cellulose microfibrils and extending from one bordered pit to the other were observed (Fig. 1, *e*). Observations of a transverse section showed that the secondary cell walls of the tracheids were heavily degraded or completely absent (Fig. 1,*f*). Some tracheids partially or completely detached from the middle lamella. Detachment of pit borders from tracheids was also observed (Fig. 1, *h*). SEM/EDX analysis of mineral particles on fossil wood revealed the presence of Si, Fe, Al, Ca, Mg, S.

SEM observations showed that although the fossil trunks were well preserved, there was severe deterioration of wood. The decay pattern observed is similar to that caused by erosion bacteria and has been described in a number of works (Kim et al., 1996; Björdal et al., 1999; Blanchette, 2000; Nilsson, Björdal, 2008; Björdal, 2012). Erosion bacteria degrade the secondary cell wall layers and deplete polysaccharides from the wood without affecting the middle lamella. In this type of attack bacteria produce troughs, which are parallel with cellulose microfibrils. However, we also observed the fungal hyphae and spores that indicate wood attacks by fungi.

According to the literature, the degradation of wood in waterlogged terrestrial and aquatic environments with a low oxygen concentration can be related to both bacterial (erosion and tunneling bacteria) and fungal attacks (soft rot fungi taxonomically related to Ascomycetes and Deuteromycetes) (Kim et al., 1996; Blanchette, 2000; Singh, 2012). The erosion bacterial decay of archeological wood is the major microbial decay form found under near-anaerobic conditions, in waterlogged environments. Erosion bacterial require only minimum oxygen concentration for their decay activities in contrast to soft rot and tunneling bacteria. Tunneling bacteria produce minute tunnels and are able to degrade all wood cell wall areas, including the highly lignified middle lamella. The wood attack by soft rot fungi result in the formation of longitudinal cavities within the secondary wall of wood cells or an erosion of the entire secondary wall. The chemical effects of soft rot attacks are preferential depletion of both hemicelluloses and cellulose; lignin is modified only to a certain extent. Striated appearance of the bacterial eroded wall distinguishes this attack from soft rot erosion (Blanchette, 2000; Björdal et al., 2000; Björdal, 2012; Singh, 2012). Our SEM results are consistent with previous findings by M. Bardet and A. Pournou (2015) and K. Nikolouli et al. (2016) who observed the patterns of decay attributed to fungi, erosion and tunneling bacteria in the fossil wood samples from the Bükkábrány area and concluded that the burial environment of the Miocene Bükkábrány fossil forest varied regarding concentration of oxygen through the time but anoxic conditions probably dominated.

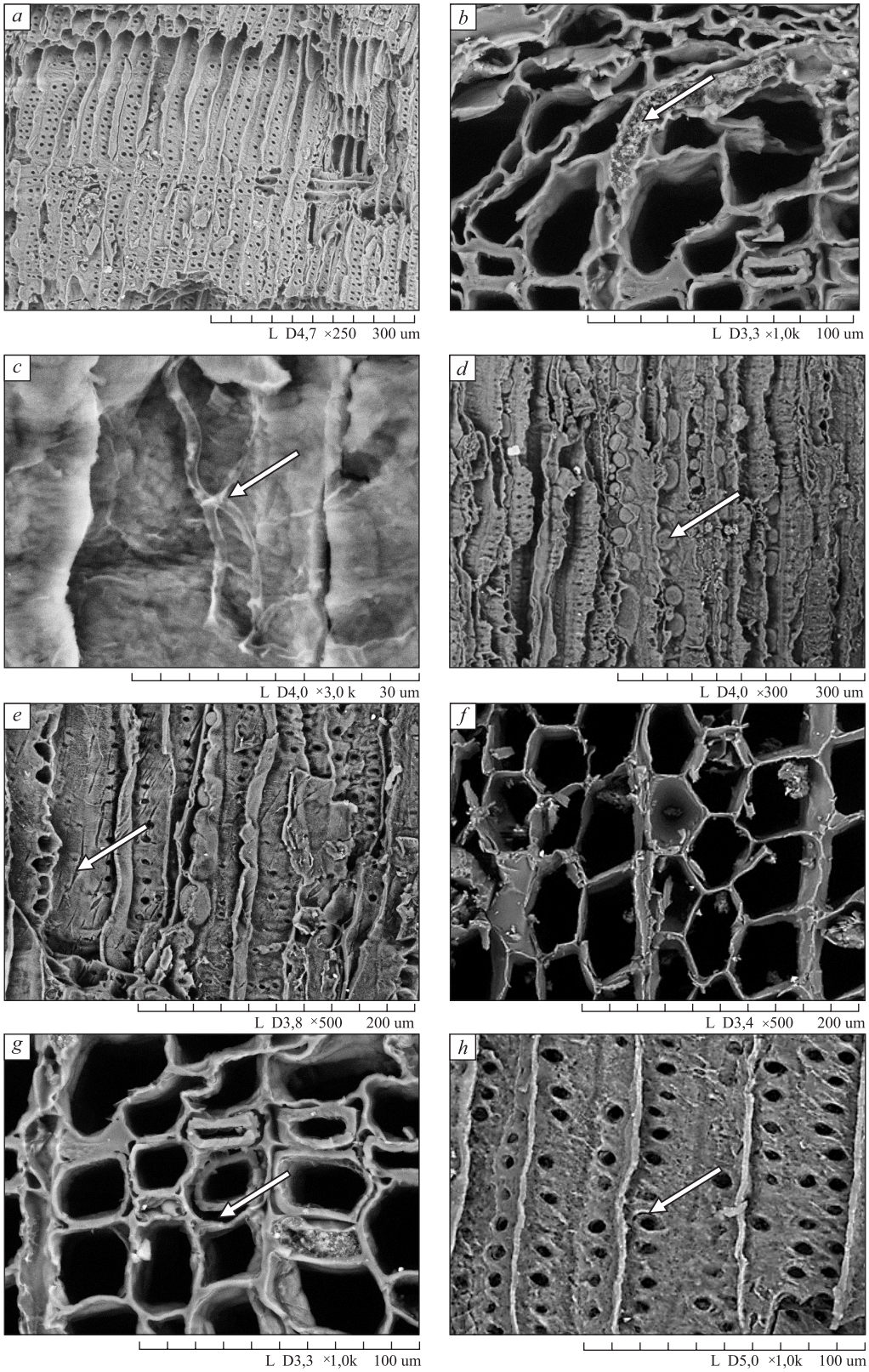

Fig. 1. SEM transverse and longitudinal sections of fossil wood showing tracheids (*a*) and ray parenchyma cells with deposits (*b*), fungal hyphae (*c*) and spores (*d*), erosion troughs (*e*), degraded secondary cell walls of the tracheids (*f*), detached tracheid (*g*) and pit border (*h*).

Thermal analysis. Figure 2 shows the thermograms obtained in an air atmosphere for fossil and recent woods.

It can be seen from the shapes of DTG curves that fossil wood demonstrated completely different thermal behavior compared to recent wood. The DTG curve of recent wood showed three peaks corresponding three successive stages of mass loss in the TG curve.

The first stage was due to the release of adsorbed water and the next two stages were mainly attributed to the thermal degradation of polysaccharides and lignin (Campanella et al., 1991; Budrugeac, Emandi, 2010; Romagnoli et al., 2018). Recent wood revealed 7.69 % of mass loss (peak at 63 °C) due to water evaporation. The slight shoulder in the DTG curve at ca 287 °C and a peak at 328 °C were related to the thermal decomposition of hemicelluloses and cellulose, respectively. There was a total mass loss of 60.24 % at this stage.

The peak at 443 °C was associated with mass loss of 30.32 % due to the thermo-oxidation of lignin. The process of the thermal degradation of recent wood finished by 502 °C. The mass loss above 502 °C was negligible. The residual mass at 700 °C (ash %) was 1.03 %. The enthalpy change (ΔH) of thermo-oxidation of recent wood was –11.41 ± 0.41 kJ/g.

DTG curve of fossil wood revealed a high heterogeneity in chemical composition and considerable overlapping the thermal decomposition stages due to the presence of degradation products (Fig. 2, *b*). To better visualize the stages of fossil wood degradation and establish the temperature intervals of mass loss, we resorted to the method of differentiating the contour of the mass loss rate $\partial^4(\mathrm{DTG})/\partial t^4 = f(t)$ (t – temperature). Then after equating the positive values of the derivative to zero, we approximated the obtained dependence by the Chebyshev polynomial of the 20th order (Fig. 2, *b*, curve *3*).

In the temperature range 25–178 °C, two peaks in the DTG curve of fossil wood were attributed to losses of different fractions of water. The broad peak at 75 °C and corresponding mass losses

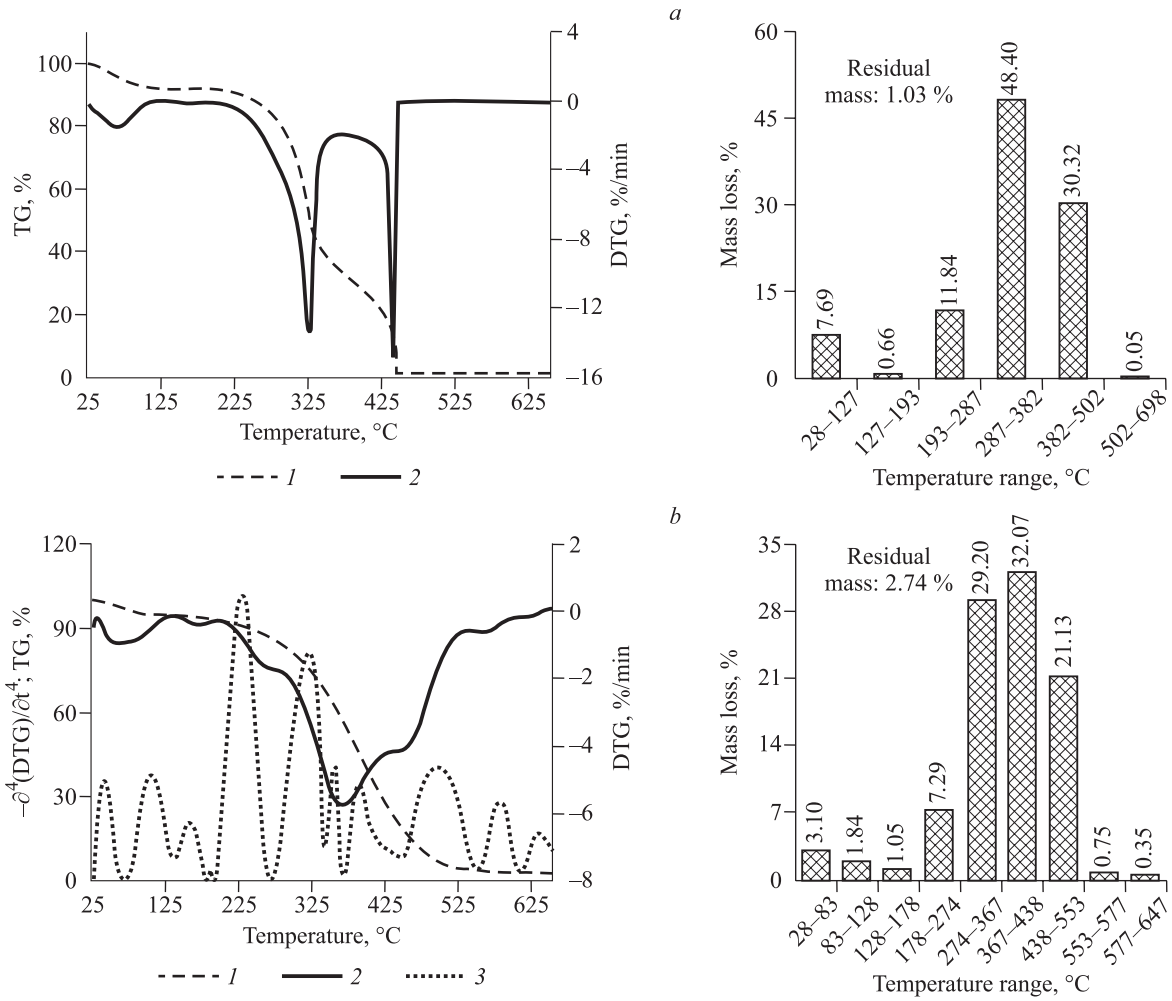

Fig. 2. Thermograms and mass losses of recent (*a*) and fossil (*b*) wood.
1 – TG curve; *2* – DTG curve; *3* – $\partial^4(\mathrm{DTG})/\partial t^4$ curve.

of 3.10 and 1.84 % were related to the release of adsorbed water from wood. The peak at 160 °C (mass loss of 1.05 %) was not observed for recent wood and likely might be due to loss of water from hydrated salts (Genestar, Pons, 2008) contained in the fossil wood sample.

The thermal degradation of the wood substance occurred above 178 °C. The DTG curve did not reveal two distinct peaks corresponding to degradation of polysaccharides and lignin like in the case of recent wood. Only one broad peak at 369 °C with two shoulders at ca 250 and 450 °C and slight mass losses above 553 °C were observed in the TG/DTG curves. The $\partial^4(DTG)/\partial t^4$ curve allowed us to distinguish six individual stages of mass loss within the interval 178–700 °C. In comparison with recent wood, the mass loss in the temperature range of 178–367 °C decreased by 40 % and mainly occurred due to the remaining cellulose. In waterlogged conditions, hemicelluloses are the first constituents lost because of their highest susceptibility to biological degradation (Romagnoli et al., 2018). Our thermogravimetry data is in agreement with the chemical investigations of M. Hámor-Vidó et al. (2010) who reported cellulose content of 18–41 % in the fossil wood samples from Bükkábrány.

At temperature range 367–700 °C, the mass loss attributed to thermo-oxidation of lignin was 79 % higher in relation to recent wood. It should be noted that the process of the thermal degradation of fossil wood continued above 500 °C. Four stages of mass loss in the $\partial^4(DTG)/\partial t^4$ curve (32.07, 21.13, 0.75 and 0.35 %) point out that lignin underwent alterations which resulted in the presence of aromatic compounds with different oxidative thermal stability. These results are consistent with the previous observations of a selective removal of polysaccharides in fossil wood and its enrichment by lignin (Fengel, 1971; Obst et al., 1991; Uçar et al., 2005; Krutul et al., 2010; Ozgenc et al., 2018). Finally, at 700 °C, fossil wood had ash content of 2.74 %. The percentage of ash in fossil wood was only slightly higher than that in recent wood. A relatively low ash content indicates that fossil wood was not permineralized (Obst et al., 1991).

The enthalpy change of combustion (thermo-oxidation) was significantly greater (–18.08 ± ± 0.82 kJ/g) for fossil wood compared to recent wood. This indicates that more heat was released likely due to the higher content of lignin (aromatic compounds) in the sample. According to the literature (Kubler, 1982; Rowell, Dietenberger, 2013; Ioelovich, 2018), lignin has the highest heat of combustion compared to cellulose and wood. O. V. Voitkevich et al. (2012) reported that the enthalpy values of combustion for hardwood and softwood lignins were found to be –21.45 and –23.50 kJ/g, respectively.

Elemental analysis. The elemental analysis revealed that recent wood contained 49.16 ± 0.28 % of total carbon (TC) and 0.19 ± 0.04 % of total nitrogen (TN), fossil wood 58.05 ± 2.33 % and 0.44 ± 0.07 %, respectively. In comparison with recent wood, fossil wood had significantly higher content of TC and a twofold increase in TN due to nitrogen immobilization (Romero et al., 2005). C/N ratio, considered as an indicator of the degree of organic matter alteration (Silva et al., 2013), was in two times lower for fossil wood compared to recent wood (132 vs. 259). This is in agreement with the literature regarding the anaerobic conditions cause a decrease of this ratio in the buried plant material and fossil wood (Gröcke, 2002; Silva et al., 2013).

Py-GC/MS. The pyrograms showed 89 peaks for recent wood and 149 peaks for fossil wood (Fig. 3).

The peak area of identified compounds accounted for 92 and 87 % of the total peak area, respectively. The identified compounds, their relative amounts and origin are listed in Table. The pyrograms of both wood samples revealed the presence of pyrolysis products of polysaccharides and lignin. Pyrolysis products were attributed to polysaccharides and lignin based on literature data (Pouwels et al., 1987; Stankiewicz et al., 1997; Łucejko et al., 2012, 2021*a*; Ház et al., 2013; Karami et al., 2013; Liaw et al., 2014; Tamburini et al., 2014, 2015; Traoré et al., 2017; González Martínez et al., 2019; SriBala et al., 2019; Subagyono et al., 2021). There were the substantial differences in the presence and the relative abundance of the individual pyrolysis products between the samples. Py-GC/MS analysis also showed that wood samples are of gymnosperm origin as indicated by the presence only guaiacyl derivatives (Saiz-Jimenez, De Leeuw, 1986; Stankiewicz et al., 1997; Van Bergen et al., 2000).

The pyrogram of recent wood revealed that pyrolysis products derived from polysaccharides and lignin represented 33 and 45 % of the total peak area, respectively. The main polysaccharide pyrolysis products were methyl glyoxal, levoglucosan, acetaldehyde, 3-methylhexanal, acetic acid, acetol, 2-oxopropanoic acid methyl ester, acetoxyacetic acid, 2-hydroxy-2-cyclopenten-1-one. The other important compounds were furfural, 1,4:3,6-dianhydro-alpha-d-glucopyranose, 2-hydroxy-3-methyl-2-cyclopenten-1-one, 2(5H)-furanone.

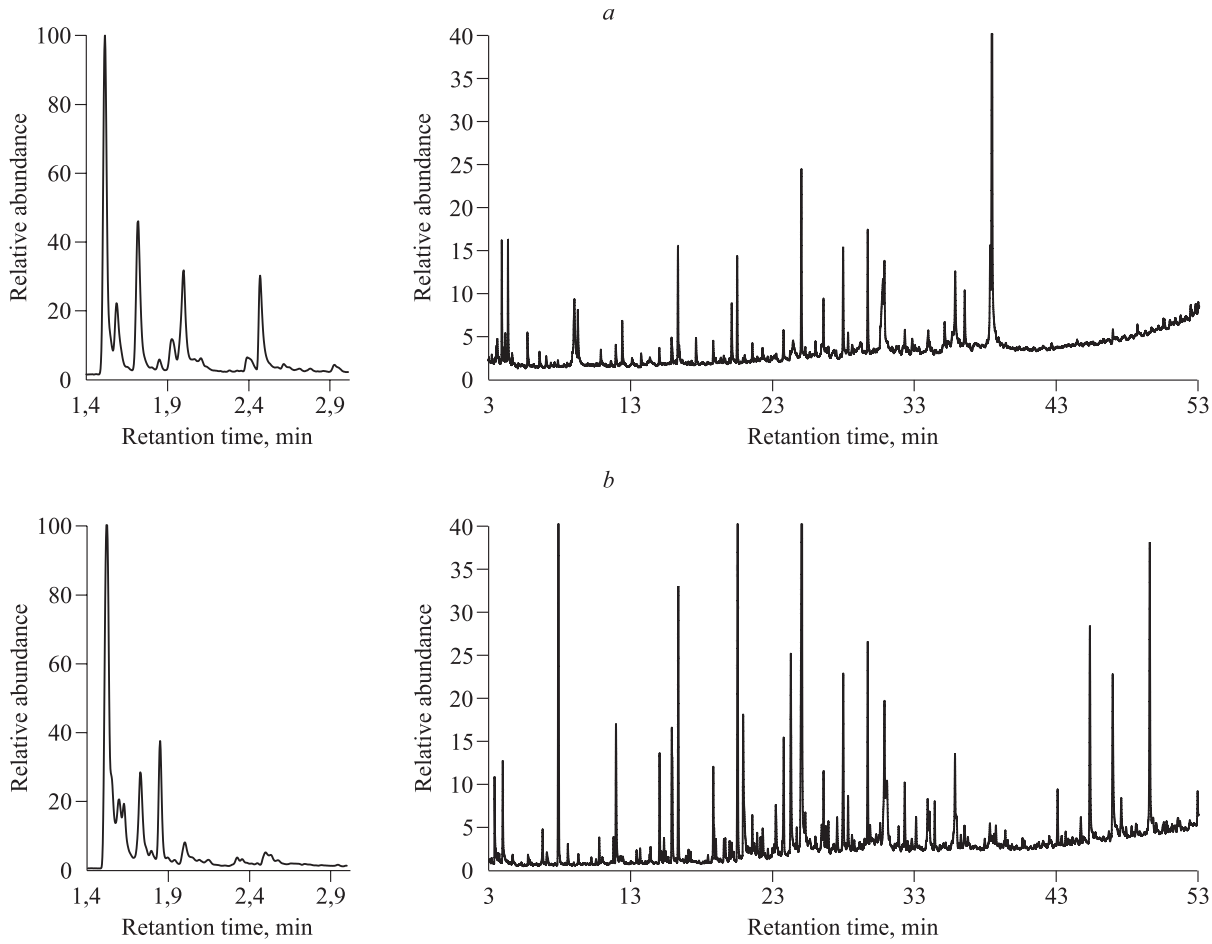

Fig. 3. Total ion current chromatograms of recent (*a*) and fossil (*b*) wood.

Pyrolysis products of lignin were mainly represented by trans-coniferyl alcohol, cis-coniferyl alcohol, guaiacol, 4-vinylguaiacol, trans-isoeugenol, dihydroconiferyl alcohol, conferyladehyde, vanillin, 4-methylguaiacol, acetovanillone, and eugenol. Coniferyl alcohol (trans- and cis-isomers) accounted for 35 % of the total lignin pyrolysis products in recent wood which agrees with the literature data for sound wood (Łucejko et al., 2021*b*). Trans-coniferyl alcohol was the dominant monomer since the lignin in conifers is based mainly on trans-coniferyl alcohol (Obst, 1983). Other lignin-compounds such as phenols, cresols, 4-ethylquaiacol were in minor abundance. The presence of trans-coniferyl alcohol in combination with relatively small amounts of phenol, 2-methylphenol, 3- and 4-methylphenol, 2,4-dimethylphenol, 3-ethylphenol, 4-ethylphenol is characteristic of nondegraded lignin (Stankiewicz et al., 1997).

Py-GC/MS of fossil wood showed a significant decrease in polysaccharide-derived compounds with regard to recent wood. The peaks deriving from polysaccharides accounted for only 3 % of the total peak area. The most of characteristic peaks of polysaccharide pyrolysis products were absent or negligible. Pyrolysis products of polysaccharides were mainly represented by levoglucosan with a combination of smaller amounts of acetaldehyde, acetic acid, and furfural. This provides evidence of a substantial degradation of hemicelluloses and cellulose in fossil wood.

A great increase in lignin pyrolysis products up to 69 % was observed. The main lignin pyrolysis products were guaiacol and guaiacyl derivatives (4-vinylguaiacol, 4-methylguaiacol, 4-ethylguaiacol, vanillin, acetovanillone), 4-methylcatechol, and catechol. It is important to note that styrene was highly abundant in fossil wood compared to recent wood. Other significant lignin-derived peaks in the pyrogram were related to the presence of phenol and phenolic compounds. A relative abundance of cresols was markedly higher than in recent wood.

We calculated the pyrolytic H/L ratio, which is a commonly used parameter to estimate the preferential loss of polysaccharides or lignin in a degraded wood sample by comparing its value with that obtained for sound wood (Tamburini et al., 2015; Zoia et al., 2017; Łucejko et al., 2021*a*). The recent

List of the identified pyrolysis products

No.	Name	Retention time (min)		Origin	Relative area (%)	
		recent wood	fossil wood		recent wood	fossil wood
1	2	3	4	5	6	7
1	Carbon dioxide	1.514	1.517		9.66	6.57
2	Acetaldehyde	1.587	1.593	Ps	2.70	0.97
3	Methanethiol	–	1.624		–	0.75
4	Methyl glyoxal	1.718	–	Ps	4.76	–
5	Oxirane, methyl-, (S)-	–	1.727		–	1.38
6	Dimethyl sulfide	–	1.794		–	0.09
7	1-Penten-3-yne	1.850	1.849		0.24	1.32
8	1.3-Diamino-2 propanol	1.927	–		1.18	–
9	Acetic acid	1.998	2.003	Ps	3.66	0.40
10	2,3-Butanediol	2.105	–	Ps	0.21	–
11	1,3-Cyclohexadiene	–	2.329	L	–	0.14
12	1,3-Cyclopentadiene, 1-methyl-	–	2.359	L	–	0.10
13	2-Butenal	2.391	–	Ps	0.61	–
14	Acetol	2.470	–	Ps	2.73	–
15	Benzene	–	2.505	Ps, L	–	0.23
16	2,3-Pentanedione	2.779	–	Ps	0.08	–
17	1,4-Dioxin, 2,3-dihydro-	2.927	-		0.30	–
18	Propylene Glycol	–	3.373		–	0.75
19	(S)-5-Hydroxymethyl-2[5H]-furanone	3.546	–	Ps	0.21	–
20	1,4-Pentadien-3-one	3.618	–		0.44	–
21	Acetic acid, (acetyoxy)-	3.931	–	Ps	1.95	–
22	Toluene	–	3.954	Ps, L	–	0.99
23	2(5H)-Furanone	4.079	–	Ps	0.21	–
24	Succindialdehyde	4.181	–	Ps	0.46	–
25	Propanoic acid, 2-oxo-, methyl ester	4.370	–	Ps	1.97	–
26	Furfural	5.741	5.737	Ps	0.82	0.13
27	Ethylbenzene	–	6.770	L	–	0.43
28	m-Xylene	–	7.071	L	–	0.26
29	4-Cyclopentene-1,3-dione	7.660	–	Ps	0.07	–
30	Styrene	7.892	7.895	L	0.11	8.29
31	Ethanol, 2-butoxy-	–	8.554		–	0.20
32	Hexanal, 3-methyl-	9.054	–	Ps	3.89	–
33	2-Cyclopente-1-one, 2-hydroxy-	9.296	–	Ps	1.54	–
34	Benzaldehyde	–	10.774	L	–	0.26
35	Butanedioic acid, cyclic hydrazide	10.921	–		0.27	–
36	alpha-Methylstyrene	–	11.783	L	–	0.25
37	Phenol	11.972	11.958	L	0.54	1.86
38	Oxazolidine, 2,2-diethyl-3-methyl-	12.433	–	Ps	0.94	–
39	Benzene, 1-methoxy-3-methyl-	–	13.415	L	–	0.14
40	Benzene, 1-propenyl-	–	13.663	L	–	0.18
41	2-Cyclopenten-1-one, 2-hydroxy-3-methyl-	13.760	–	Ps	0.37	–
42	Benzaldehyde, 2-hydroxy-	–	14.336	L	–	0.08
43	o-Cresol	15.047	15.035	L	0.39	1.13
44	Benzenemethanol, alpha-methyl-	–	15.176		–	0.09
45	Acetophenone	–	15.352	L	–	0.23
46	p-Cresol	15.906	15.900	L	0.87	1.37
47	m-Cresol	–	15.930	L	–	0.92
48	Guaiacol	16.360	16.364	L	2.29	2.95
49	Pentanal	16.446	–	Ps	0.43	–

Table continuation

1	2	3	4	5	6	7
50	Phenol, 2,6-dimethyl-	–	17.082	L	–	0.18
51	2,5-Dimethylanisole	–	17.221	L	–	0.11
52	2,4(3H,5H)-Furandione, 3-methyl-	17.635	–	Ps	0.68	–
53	Phenol, 2-ethyl-	–	18.461	L	–	0.07
54	Phenol, 2,4-dimethyl-	18.849	18.837	L	0.59	0.47
55	Phenol, 2,5-dimethyl-	–	18.893	L	–	0.26
56	Benzaldehyde,2-hydroxy-5-methyl-	19.019	19.017	L	0.13	0.20
57	Phenol, 4-ethyl-	19.594	19.588	L	0.13	0.19
58	Phenol, 3,4-dimethyl-	19.690	19.683	L	0.07	0.18
59	Phenol, 2-methoxy-3-methyl-	19.987	19.985	L	0.12	0.22
60	4-Methylguaiacol	20.541	20.557	L	2.18	5.19
61	Catechol	–	20.946	L	–	2.55
62	1,4:3,6-Dianhydro-alpha-d-glucopyranose	21.072	–	Ps	0.20	–
63	Benzofuran, 2,3-dihydro-	21.609	21.593	Ps, L	0.43	0.38
64	Sulfurous acid, cyclohexylmethyl nonyl ester	–	22.171		–	0.18
65	Phenol, 3-ethyl-5-methyl-	22.323	22.324	L	0.31	0.40
66	Phenol, 2,3,5,6-tetramethyl-	22.697	22.692	L	0.09	0.10
67	Benzoic acid, 2-propenyl ester	–	23.018		–	0.08
68	3-Methylcatechol	–	23.247	L	–	0.69
69	4,7-Methano-1H-indenol, hexahydro-	–	23.711		–	0.12
70	4-Ethylguaiacol	23.809	23.810	L	0.67	1.40
71	2-Allylphenol	24.276	–	L	0.23	
72	4-Methylcatechol	–	24.312	L	–	2.87
73	Benzofuran, 2,3-dihydro-2-methyl-	–	24.732	L	–	0.20
74	4-Vinylguaiacol	25.069	25.091	L	3.75	9.62
75	3-Methoxy-5-methylphenol	25.344	25.339	L	0.17	0.25
76	Phenol, 4-(2-propenyl)-	26.060	26.049	L	0.28	0.09
77	Eugenol	26.625	26.625	L	1.12	0.71
78	Phenol, 2-methoxy-4-propyl-	26.967	26.968	L	0.16	0.33
79	4-Ethylcatechol	–	27.585	L	–	0.48
80	Vanillin	28.013	28.021	L	2.47	2.43
81	trans-Isoeugenol	28.360	28.360	L	0.35	0.52
82	Phenol, 2-methyl-6-(2-propenyl)-	28.651	28.636	L	0.33	0.23
83	trans-Isoeugenol	29.745	29.747	L	2.85	2.25
84	Dimethyl phthalate	–	29.915		–	0.22
85	Levoglucosan	30.822	31.109	Ps	4.56	1.95
86	Acetovanillone	30.926	30.933	L	2.24	2.74
87	Vanillic acid methyl ester	–	31.933	L	–	0.21
88	2-Propanone, 1-(4-hydroxy-3-methoxyphenyl)-	32.365	32.364	L	0.58	0.87
89	1-Propanone, 1-(4-hydroxy-3-methoxyphenyl)-	–	33.982	L	–	0.94
90	Butyrovanillone	–	34.118	L	–	0.50
91	2,2,4-Trimethyl-1,3-pentanediol diisobutyrate	–	34.482		–	0.49
92	Dihydroconiferyl alcohol	35.918	35.917	L	2.79	1.34
93	7-Methoxy-1-naphthol	–	36.328		–	0.13
94	cis-Coniferyl alcohol	36.587	36.587	L	1.54	0.41
95	Coniferylaldehyde	38.384	38.385	L	2.63	0.27
96	trans-Coniferyl alcohol	38.511	38.499	L	14.14	0.07
97	Diallyl phthalate	-	38.807		–	0.21
98	Benzene, 1’1-(1,3-butadienylidene)bis-	–	40.691		–	0.13
99	Phenol, 2,2’-methylenebis-	–	44.810	L	–	0.44

End of table

1	2	3	4	5	6	7
100	Phenol, 2-[(4-hydroxyphenil)methyl]-	–	45.449	L	–	2.93
101	Phenol, 4,4'-methylenebis-	–	47.061	L	–	2.72
102	Phenol, 4,4'-(1-methylethylidene)bis-	–	49.680	L	–	4.03
103	Ferruginol	53.192	53.185		0.79	0.19
104	Cyclohexane, 1,3,5-triphenyl-	–	55.251		–	0.49
105	(E)-3'3-Dimethoxy-4,4'-dihydroxystilbene	57.952	57.947	L	1.23	0.31
106	3,4-Divanillyltetrahydrofuran	–	60.973		–	0.32
Sum of identified compounds					91.71	87.32
Sum of polysaccharide pyrolysis compounds					33.05	3.45
Sum of lignin pyrolysis compounds					45.35	68.56
Holocellulose/lignin (H/L)					0.7	0.1

Note. The relative area was expressed as a percentage of the total area of the peaks detected in the pyrogram. The holocellulose/lignin (H/L) is defined as the ratio between the relative abundances of holocellulose (cellulose and hemicelluloses) and lignin pyrolysis products (Łucejko et al., 2021*a*).

and fossil woods had H/L ratios 0.7 and 0.1, respectively (Table). This highlights a preferential loss of polysaccharides in fossil wood from Bükkábrány.

In order to provide more information on chemical alterations in lignin we summarized the peak areas of the pyrolysis products assigned to following categories: monomers (coniferyl alcohol), long chain compounds (guaiacyl units with modified C3 alkyl chains), short chain compounds (guaiacyl units with up to C2 alkyl chains), carbonyl compounds (compounds containing aldehyde and ketone functionalities), carboxyl compounds (acids and esters), demethylated/demethoxylated compounds (guaiacyl units in which the methoxy groups on the aromatic rings had undergone alteration), and others (Tamburini et al., 2015, 2016; Braovac et al., 2016; Łucejko et al., 2020, 2021*b*).

In recent wood, monomers accounted for 35 %, long chain compounds 10 %, short chain compounds 20 %, carbonyl compounds 16 %, others 20 %, carboxyl and demethylated/demethoxylated compounds were not detected. The distribution of lignin pyrolysis products in fossil wood was different. Monomers constituted for only ca 1 %; long chain compounds 5 %, short chain compounds 28 %, carbonyl compounds 8 %, carboxyl compounds 0.3 %, demethylated/demethoxylated compounds 10 %, others 49 %.

Although lignin is generally less susceptible to degradation processes in the burial environment, especially in waterlogged conditions, compared to cellulose and hemicelluloses it also undergoes chemical changes, which can involve demethylation, oxidation, and depolymerisation (Saiz-Jimenez, De Leeuw, 1986; Tamburini et al., 2016; Łucejko et al., 2021*b*). The results of Py-GC-MS of fossil wood showed that not only the relative amount of lignin-derived pyrolysis products substantially increased but also their chemical composition changed. Coniferyl alcohol is characteristic of an unaltered gymnosperm lignin and its strong decrease indicates the structural changes in lignin due to degradation (Saiz-Jimenez, De Leeuw, 1986; Łucejko et al., 2021*b*). The higher relative abundance of shortened side chain pyrolysis products compared to lignin monomers is connected to the depolymerisation of lignin (Tamburini et al., 2016; Łucejko et al., 2021*b*). The formation of catechol-type compounds (catechol, 3-methylcatechol, 4-methylcatechol, 4-ethylcatechol) also reflects the lignin degradation. Catechol is the main degradation product of gymnospermous lignin arising via demethylation of the methoxyl group (Van Bergen et al., 2000). Demethylation occurs in degradation pathways initiated by fungi or bacteria and results in lignin units with hydroxyl groups, which are more reactive and thus susceptible to further reactions (Łucejko et al., 2021*a*). The relative abundance of catechol-like and phenol-like structures was observed in plant materials (degraded wood, coalified logs) at different stages of the coalification process (Hatcher et al., 1988, 1989). A significant decrease in the relative amount of carbonyl compounds in fossil wood points to alteration of lignin. This also reflects the absence of the oxidizing conditions because the oxidation of lignin results in an increase in carbonyl and carboxyl functionalities (Łucejko et al., 2021*b*). Moreover, a low relative amount of oxidized phenols such as vanillic acid methyl ester in fossil wood as well

indicates an anoxic burial history (Saiz-Jimenez et al., 1987).

The fossil wood showed higher abundance of cresols, phenol and monocyclic aromatic hydrocarbons (benzene, toluene, m-xylene, styrene) compared to recent wood. Phenolic compounds such as phenol, 2,2′-methylenebis-; phenol, 2-[(4-hydroxyphenil)methyl]-; phenol, 4,4′-methylenebis-; phenol, 4,4′-(1-methylethylidene)bis- and polycyclic aromatic hydrocarbons (7-methoxy-1-naphthol) were not encountered in recent wood. D. Shen et al. (2015) reported that the presence of phenol-type and cresol-type compounds is related to the demethoxylation of guaiacol-type compounds. It should also be noted that a high relative abundance of styrene in the pyrolysates of fossil wood indicates lignin degradation (Nierop et al., 2001).

The peak of methanethiol in the pyrogram of fossil wood reflects the presence of sulphur-containing compounds. This is in agreement with observations of J. Guo et al. (2019) who reported that methanethiol can be a result of the enrichment of organic sulfur produced by sulfate reducing bacteria.

CONCLUSION

In this study, the methods of thermal analysis and analytical pyrolysis were used in order to provide more information about degradation of the unique fossil wood from the Bükkábrány area. Thermal analysis of fossil wood showed a high heterogeneity of wood substance, a significant degradation of polysaccharides and enrichment by lignin including more thermally stable components (> 500 °C), a larger enthalpy change (ΔH) of combustion compared to recent wood. Py-GC/MS results were in agreement with thermal analysis indicating a preferential loss of polysaccharides. Polysaccharide pyrolysis products were mainly represented by levoglucosan. Other polysaccharide-derived compounds were not detected or were present in minor quantities. Among lignin pyrolysis products, a significantly low abundance of lignin monomers, an increase in short side-chain compounds and presence of demethylated/demethoxylated units in fossil wood provided evidence of lignin alteration (degradation). Thus, obtained results showed that fossil wood, which had been exposed to the burial environment for 7 million years, had significant changes in the chemical composition.

The work was carried out as part of project No. TKP2021-NKTA-43 and in the frame of cooperation agreement on academic and research between V. N. Sukachev Institute of Forest Russian Academy of Sciences, Siberian Branch – separate subdivision of Federal Research Center «Krasnoyarsk Science Center Russian Academy of Sciences, Siberian Branch» and University of Sopron. This project has been implemented with the support provided by the Ministry of Innovation and Technology of Hungary from the National Research, Development and Innovation Fund, financed under the TKP2021-NKTA funding scheme.

The authors thank thieir collegues from the International laboratory «Ecophysiology of biogeocenosis of the cryolithic zone», V. N. Sukachev Institute of Forest SB RAS, for undertaking the elemental analysis.

REFERENCES

Bardet M., Pournou A. Fossil wood from the Miocene and Oligocene epoch: chemistry and morphology // Magn. Reson. Chem. 2015. V. 53. Iss. 1. P. 9–14.

Björdal C. G. Microbial degradation of waterlogged archaeological wood // J. Cult. Herit. 2012. V. 13. Iss. 3. Suppl. P. 118–122.

Björdal C. G., Daniel G., Nilsson T. Depth of burial, an important factor in controlling bacterial decay of waterlogged archaeological poles // Int. Biodeterior. Biodegr. 2000. V. 45. Iss. 1–2. P. 15–26.

Björdal C. G., Nilsson T., Daniel G. Microbial decay of waterlogged archaeological wood found in Sweden. Applicable to archaeology and conservation // Int. Biodeterior. Biodegr. 1999. V. 43. Iss. 1–2. P. 63–73.

Blanchette R. A. A review of microbial deterioration found in archaeological wood from different environments // Int. Biodeterior. Biodegr. 2000. V. 46. Iss. 3. P. 189–204.

Braovac S., Tamburini D., Łucejko J. J., McQueen C., Kutzke H., Colombini M. P. Chemical analyses of extremely degraded wood using analytical pyrolysis and inductively coupled plasma atomic emission spectroscopy // Microchem. J. 2016. V. 124. P. 368–379.

Budrugeac P., Emandi A. The use of thermal analysis methods for conservation state determination of historical and/or cultural objects manufactured from lime tree wood // J. Therm. Anal. Calorim. 2010. V. 101. Iss. 3. P. 881–886.

Campanella L., Tomassetti M., Tomellini R. Thermoanalysis of ancient, fresh and waterlogged woods // J. Therm. Anal. 1991. V. 37. Iss. 8. P. 1923–1932.

Cavallaro G., Donato D. I., Lazzara G., Milioto S. A comparative thermogravimetric study of waterlogged archaeological and sound woods // J. Therm. Anal. Calorim. 2011. V. 104. Iss. 2. P. 451–457.

Colombini M. P., Orlandi M., Modugno F., Tolppa E.-L., Sardelli M., Zoia L., Crestini C. Archaeological wood characterization by PY/GC/MS, GC/MS, NMR and GPC techniques // Microchem. J. 2007. V. 85. Iss. 1. P. 164–173.

Donato D. I., Lazzara G., Milioto S. Thermogravimetric analysis: a tool to evaluate the ability of mixtures in consolidating waterlogged archaeological woods // J. Therm. Anal. Calorim. 2010. V. 101. Iss. 3. P. 1085–1091.

Erdei B., Dolezych M., Hably L. The buried Miocene forest at Bükkábrány, Hungary // Rev. Palaeobot. Palynol. 2009. V. 155. Iss. 1–2. P. 69–79.

Fengel D. Chemische und elektronmikroskopische Untersuchung eines fossilen Fichtenholzes // Holz Roh Werkst. 1971. V. 29. Iss. 8. P. 305–314.

Genestar C., Pons C. Analytical characterization of biodegraded wood from a 15th century Spanish cloister // Microchim Acta. 2008. V. 162. Iss. 3. P. 333–339.

Ghalibaf M., Lehto J., Alén R. Fast pyrolysis of hot-water-extracted and delignified Norway spruce (*Picea abies*) sawdust by Py-GC/MS // Wood Sci. Technol. 2019. V. 53. Iss. 1. P. 87–100.

González Martínez M., Ohra-aho T., da Silva Perez D., Tamminen T., Dupont C. Influence of step duration in fractionated Py-GC/MS of lignocellulosic biomass // J. Anal. Appl. Pyrol. 2019. V. 137. P. 195–202.

Gröcke D. R. The carbon isotope composition of ancient CO_2 based on higher-plant organic matter // Philos. Trans. Ser. A. Math. Phys. Eng. Sci. 2002. V. 360. Iss. 1793. P. 633–658.

Gryc V., Sakala J. Identification of fossil trunks from Bükkábrány newly installed in the visitor centre of the Ipolytarnóc Fossils Nature Reserve (Novhrad-Nógrád Geopark) in northern Hungary // Acta Univ. Agr. Silv. Mendel. Brun. 2010. V. 58. Iss. 5. P. 117–122.

Guleria J. S., Awasthi N. Fossil wood and their significance // Curr. Sci. 1997. V. 72. N. 4. P. 248–254.

Guo J., Xiao L., Han L., Wu H., Yang T., Wu S., Yin Y. Deterioration of the cell wall in waterlogged wooden archeological artifacts, 2400 years old // IAWA J. 2019. V. 40. Iss. 4. P. 820–844.

Hámor-Vidó M., Hofmann T., Albert L. In situ preservation and paleoenvironmental assessment of Taxodiacea fossil trees in the Bükkalja Lignite Formation, Bükkábrány open cast mine, Hungary // Int. J. Coal Geol. 2010. V. 81. Iss. 4. P. 203–210.

Hatcher P. G., Lerch H. E., Kotra R. K., Verheyen T. V. Pyrolysis g.c.-m.s. of a series of degraded woods and coalified logs that increase in rank from peat to subbituminous coal // Fuel. 1988. V. 67. Iss. 8. P. 1069-1075.

Hatcher P. G., Lerch H. E., Verheyen T. V. Organic geochemical studies of the transformation of gymnospermous xylem during peatification and coalification to subbituminous coal // Int. J. Coal Geol. 1989. V. 13. Iss. 1–4. P. 65-97.

Ház A., Jablonský M., Orságová A., Šurina I. Characterization of lignins by Py-GC/MS // Renewable energy sources: Proc. 4nd Int. Conf. High Tatras. Slovak Rep., 2013.

Ioelovich M. Thermodynamics of biomass-based solid fuels // Acad. J. Polym. Sci. 2018. V. 2. Iss. 1. P. 555–557.

Karami L., Schmidt O., Fromm J., Klinberg A., Schmitt U. Wood decay characterization of a naturally infected oak wood bridge using PY-GC/MS // Wood Res. 2013. V. 58. N. 4. P. 591–598.

Kázmér M. The Miocene Bükkábrány fossil forest in Hungary – field observations and project outline // Hantkeniana. 2008. V. 6. Iss. 6. P. 229-244.

Kázmér M. Structure of the 7 Ma Bükkábrány fossil forest in Hungary // Jap. J. Histor. Bot. 2011. V. 19. Iss. 1–2. P. 47–54.

Kim Y. S., Singh A. P., Nilsson T. Bacteria as important degraders in waterlogged archaeological woods // Holzforschung. 1996. V. 50. N. 5. P. 389–392.

Krutul D., Radomski A., Zawadzki J., Zielenkiewicz T., Antczak A. Comparison of the chemical composition of the fossil and recent oak wood // Wood Res. 2010. V. 55. N. 3. P. 113–120.

Kubler H. Heat release in thermally disintegrating wood // Wood and Fiber. 1982. V. 14. N. 3. P. 166–177.

Liaw S. S., Perez V. H., Zhou S., Rodriguez-Justo O., Garcia-Perez M. Py-GC/MS studies and principal component analysis to evaluate the impact of feedstock and temperature on the distribution of products during fast pyrolysis // J. Anal. Appl. Pyrol. 2014. V. 109. P. 140–151.

Łucejko J. J., McQueen C. M., Sahlstedt M., Modugno F., Colombini M. P., Braovac S. Comparative chemical investigations of alum treated archaeological wood from various museum collections // Herit. Sci. 2021*a*. V. 9. Iss. 1. Article number: 69. 17 p.

Łucejko J. J., Modugno F., Ribechini E., del Río J. C. Characterisation of archaeological waterlogged wood by pyrolytic and mass spectrometric techniques // Anal. Chim. Acta. 2009. V. 654. Iss. 1. P. 26–34.

Łucejko J. J., Modugno F., Ribechini E., Tamburini D., Colombini M. P. Analytical instrumental techniques to study archaeological wood degradation // Appl. Spectrosc. Rev. 2015. V. 50. Iss. 7. P. 584–625.

Lucejko J. J., Tamburini D., Zborowska M. M., Babiński L., Modugno F., Colombini M. P. Oak wood degradation processes induced by the burial environment in the archaeological site of Biskupin (Poland) // Herit. Sci. 2020. V. 8. Article number: 44. 12 p.

Lucejko J. J., Tamburini D., Modugno F., Ribechini E., Colombini M. P. Analytical pyrolysis and mass spectrometry to characterize lignin in archaeological wood // Appl. Sci. 2021*b*. V. 11. Iss. 1. Article number: 240. 25 p.

Łucejko J. J., Zborowska M., Modugno F., Colombini M. P., Prądzyński W. Analytical pyrolysis vs. classical wet chemical analysis to assess the decay of archaeological waterlogged wood // Anal. Chim. Acta. 2012. V. 745. P. 70–77.

Mustoe G. E. Non-mineralized fossil wood // Geosciences. 2018. V. 8. Iss. 6. P. 223.

Nierop K. G., Pulleman M. M., Marinissen J. C. Management induced organic matter differentiation in grassland and arable soil: a study using pyrolysis techniques // Soil Biol. Biochem. 2001. V. 33. N. 6. P. 755–764.

Nikolouli K., Pournou A., McConnachie G., Tsiamis G., Mossialos D. Prokaryotic diversity in biodeteriorated wood coming from the Bükkábrány fossil forest // Int. Biodeterior. Biodegr. 2016. V. 108. P. 181–190.

Nilsson T., Björdal C. Culturing wood-degrading erosion bacteria // Int. Biodeterior. Biodegr. 2008. V. 61. Iss. 1. P. 3–10.

Obst J. R. Analytical pyrolysis of hardwood and softwood lignins and its use in lignin type determinations hardwood vessel elements // J. Wood Chem. Technol. 1983. V. 3. Iss. 4. P. 377–397.

Obst J. R., McMillan N. J, Blanchette R. A., Christensen D. J., Faix O., Han J. S., Kuster T. A., Landucci L. L., Newman R. H., Pettersen R. C., Schwandt V. H., Wesolowski M. F. Characterization of Canadian Arctic fossil woods // Tertiary fossil forests of the Geodetic Hills, Axel Heiberg Island, Arctic Archipelago / R. L. Christie, N. J. McMillan (Eds.). Geol. Surv. Can. 1991. Bull. 403. P. 123–146.

Ozgenc O., Durmaz S., Serdar B., Boyaci I. H., Eksi-Kocak H., Öztürk M. Characterization of fossil Sequoioxylon wood using analytical instrumental techniques // Vibr. Spectrosc. 2018. V. 96. P. 10–18.

Pouwels A. D., Tom A., Eijkel G. B., Boon J. J. Characterization of beech wood and its holocellulose and xylan fractions by pyrolysis-gas chromatography-mass spectrometry // J. Anal. Appl. Pyrol. 1987. V. 11. P. 417–436.

Romagnoli M., Galotta G., Antonelli F., Sidoti G., Humar M., Kržišnik D., Čufar K., Petriaggi B. D. Micro-morphological, physical and thermogravimetric analyses of waterlogged archaeological wood from the prehistoric village of Gran Carro (Lake Bolsena-Italy) // J. Cult. Herit. 2018. V. 33. P. 30–38.

Romero L. M., Smith III T. J., Fourqurean J. W. Changes in mass and nutrient content of wood during decomposition in a south Florida mangrove forest // J. Ecol. 2005. V. 93. Iss. 3. P. 618–631.

Rowell R. M., Dietenberger M. A. Thermal properties, combustion, and fire retardancy of wood // Handbook of wood chemistry and wood composites / R. M. Rowell (Ed.). 2nd ed. New York: CRC Press, 2013. P. 127–149.

Saiz-Jimenez C., Boon J. J., Hedges J. I., Hessels J. K., De Leeuw J. W. Chemical characterization of recent and buried woods by analytical pyrolysis: Comparison of pyrolysis data with 13C NMR and wet chemical data // J. Analyt. Appl. Pyrol. 1987. V. 11. P. 437–450.

Saiz-Jimenez C., De Leeuw J. W. Lignin pyrolysis products: Their structures and their significance as biomarkers // Org. Geochem. 1986. V. 10. Iss. 4–6. P. 869–876.

Shen D., Jin W., Hu J., Xiao R., Luo K. An overview on fast pyrolysis of the main constituents in lignocellulosic biomass to valued-added chemicals: Structures, pathways and interactions // Renew. Sust. Energ. Rev. 2015. V. 51. P. 761–774.

Silva R. L., Duarte L. V., Filho J. G. Optical and geochemical characterization of Upper Sinemurian (Lower Jurassic) fossil wood from the Lusitanian Basin (Portugal) // Geochem. J. 2013. V. 47. Iss. 5. P. 489–498.

Singh A. P. A review of microbial decay types found in wooden objects of cultural heritage recovered from buried and waterlogged environments // J. Cult. Herit. 2012. V. 13. Iss. 3. Suppl. P. 16–20.

SriBala G., Toraman H. E., Symoens S., Déjardin A., Pilate G., Boerjan W., Ronsse F., Van Geem K. M., Marin G. B. Analytical Py-GC/MS of genetically modified poplar for the increased production of bio-aromatics // Comput. Struct. Biotechnol. J. 2019. V. 17. P. 599–610.

Stankiewicz B. A., Mastalerz M., Kruge M. A., van Bergen P. F., Sadowska A. A comparative study of modern and fossil cone scales and seeds of conifers: A geochemical approach // New Phytol. 1997. V. 135. Iss. 2. P. 375–393.

Subagyono R. R. D. J. N., Qi Y., Chaffee A. L., Amirta R., Marshall M. Pyrolysis-GC/MS analysis of fast growing wood *Macaranga* species // Indones. J. Sci. Technol. 2021. V. 6. N. 1. P. 141–158.

Tamburini D., Łucejko J. J., Modugno F., Colombini M. P. Characterisation of archaeological waterlogged wood from Herculaneum by pyrolysis and mass spectrometry // Int. Biodeterior. Biodegr. 2014. V. 86. Part B. P. 142–149.

Tamburini D., Łucejko J. J., Zborowska M., Modugno F., Prądzyński W., Colombini M. P. Archaeological wood degradation at the site of Biskupin (Poland): Wet chemical analysis and evaluation of specific Py-GC/MS profiles // J. Analyt. Appl. Pyrol. 2015. V. 115. P. 7–15.

Tamburini D., Łucejko J. J., Ribechini E., Colombini M. P. New markers of natural and anthropogenic chemical alteration of archaeological lignin revealed by in situ pyrolysis/silylation-gas chromatography-mass spectrometry // J. Analyt. Appl. Pyrol. 2016. V. 118. P. 249–258.

Tomassetti M., Campanella L., Tomellini R., Meucci C. Thermogravimetric analysis of fresh and archeological waterlogged woods // Thermochim. Acta. 1987. V. 117. P. 297–315.

Traoré M., Kaal J., Cortizas A. M. Application of FTIR spectroscopy to the characterization of archeological wood // Spectrochim. Acta Part A: Mol. Biomol. Spectrosc. 2016. V. 153. P. 63–70.

Traoré M., Kaal J., Cortizas A. M. Potential of pyrolysis-GC–MS molecular fingerprint as a proxy of Modern Age Iberian shipwreck wood preservation // J. Anal. Appl. Pyrol. 2017. V. 126. P. 1–13.

Uçar G., Meier D., Faix O., Wegener G. Analytical pyrolysis and FTIR spectroscopy of fossil *Sequoiadendron giganteum* (Lindl.) wood and MWLs isolated hereof // Holz Roh Werkst. 2005. V. 63. Iss. 1. P. 57–63.

Van Bergen P. F., Poole I., *Ogilvie T. M., Caple* C., *Evershed R. P.* Evidence for demethylation of syringyl moieties in archaeological wood using pyrolysis-gas chromatography/mass spectrometry // Rapid Commun. Mass Spectrom. 2000. V. 14. Iss. 2. P. 71–79.

Voitkevich O. V., Kabo G. J., Blokhin A. V., Paulechka Y. U., Shishonok M. V. Thermodynamic properties of plant biomass components. Heat capacity, combustion energy, and gasification equilibria of lignin // J. Chem. Eng. Data. 2012. V. 57. Iss. 7. P. 1903–1909.

Zoia L., Tamburini D., Orlandi M., Łucejko J. J., Salanti A., Tolppa E.-L., Modugno F., Colombini M. P. Chemical characterisation of the whole plant cell wall of archaeological wood: an integrated approach // Analyt. Bioanalyt. Chem. 2017. V. 409. Iss. 17. P. 4233–4245.

ТЕРМИЧЕСКИЙ АНАЛИЗ И ПИРОЛИТИЧЕСКАЯ ГАЗОВАЯ ХРОМАТО-МАСС-СПЕКТРОМЕТРИЯ ИСКОПАЕМОЙ ДРЕВЕСИНЫ ИЗ МЕСТНОСТИ БЮККАБРАНИ, ВЕНГРИЯ

О. А. Шапченкова[1], С. Р. Лоскутов[1], М. А. Пляшечник[1], З. Пастори[2]

[1] *Институт леса им. В. Н. Сукачева СО РАН – обособленное подразделение ФИЦ КНЦ СО РАН 660036, Красноярск, Академгородок, 50/28*

[2] *Университет Шопрона*
Венгрия, 9400, Шопрон, ул. Байчи-Жилински, 4

E-mail: shapchenkova@mail.ru, lsr@ksc.krasn.ru, lilwood@ksc.krasn.ru, pasztory.zoltan@uni-sopron.hu

Ископаемая древесина возрастом около 7 млн лет из Бюккабрани (Венгрия) была проанализирована с помощью термогравиметрии (ТГ), дифференциальной сканирующей калориметрии (ДСК) и пиролитической газовой хромато-масс-спектрометрии (Пи-ГХ/МС) для оценки изменения ее химического состава. В качестве контроля был взят образец древесины таксодиума двурядного (болотного кипариса обыкновенного) (*Taxodium distichum* (L.) Rich.) из Западной Венгрии. Ископаемая древесина характеризовалась более высоким содержанием общего углерода (58.05 %) и общего азота (0.44 %) по сравнению с современной древесиной. ТГ ископаемой древесины показала высокую неоднородность древесинного вещества, значительную потерю полисахаридов и обогащение лигнином, включая более термостабильные компоненты (> 500 °C). Изменение энтальпии (ΔH) сгорания (термоокисления) ископаемой древесины было значительно больше, чем современной древесины (–18.08 против –11.41 кДж/г). Пи-ГХ/МС ископаемой древесины показала значительное уменьшение продуктов пиролиза полисахаридов и увеличение продуктов пиролиза лигнина по сравнению с современной древесиной. Пиролитическое отношение H/L свидетельствует о преимущественной потере полисахаридов в ископаемой древесине. Продукты пиролиза полисахаридов встречались редко и были представлены в основном левоглюкозаном. Лигнин также претерпел существенные изменения. Резкое уменьшение доли мономеров, увеличение доли соединений с короткой боковой цепью и присутствие деметилированных/деметоксилированных соединений в составе продуктов пиролиза лигнина указывает на изменение (деградацию) лигнина. Кроме того, отмечено высокое содержание стирола, крезолов, фенола и фенольных соединений.

Ключевые слова: *термогравиметрия, дифференциальная сканирующая калориметрия, аналитический пиролиз, оценка изменения химического состава ископаемой древесины, таксодиум двурядный (Taxodium distichum (L.) Rich.), Западная Венгрия.*

Shapchenkova O. A., Loskutov S. R., Plyashechnik M. A., Pásztory Z. Thermal analysis and pyrolysis-gas chromatography/mass spectrometry of fossil wood from of Bükkábrány, Hungary (*Шапченкова О. А., Лоскутов С. Р., Пляшечник М. А., Пастори З.* Термический анализ и пиролитическая газовая хромато-масс-спектрометрия ископаемой древесины из местности Бюккабрани, Венгрия) // Сибирский лесной журнал. 2022. № 5. С. 56–69 (на английском языке, реферат на русском).